Mixtures of Alcohols and Water confined in Mesoporous Silica: A Combined Solid-State NMR and Molecular Dynamics Simulation Study

Bharti Kumari,[†] Martin Brodrecht,[†] Hergen Breitzke,[†] Mayke Werner,[†] Bob Grünberg,[‡] Hans-Heinrich Limbach,[‡] Sandra Forg,[§] Elvira P. Sanjon,[§] Barbara Drossel,*[,§] Torsten Gutmann,*[,†] and Gerd Buntkowsky*[,†]

[†]Eduard-Zintl Institut für Anorganische und Physikalische Chemie, Technische Universität Darmstadt, Alarich-Weiss-Str. 8, D-64287 Darmstadt, Germany

[‡]Institut für Chemie und Biochemie, Freie Universität Berlin, Takustrasse 3, 14195 Berlin, Germany

[§]Institut für Festkörperphysik, Technische Universität Darmstadt, Hochschulstraße 6, 64289 Darmstadt, Germany

Ⓢ *Supporting Information*

ABSTRACT: The behavior of mixtures of 1-octanol with water with different molar ratios confined inside the mesoporous silica SBA-15 was investigated by a combination of solid-state NMR spectroscopy and molecular dynamics (MD) simulations. Two-dimensional $^1H-^{29}Si$ FSLG-HET-COR NMR spectra revealed the orientation of 1-octanol relative to the pore walls. These arrangements are in good agreement with the preferred structures found by MD. In addition, MD simulations also shed light on molecular orientations and interactions in the pore center region, which are not resolvable by solid-state NMR.
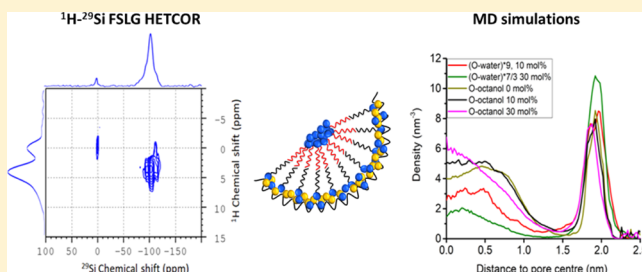
1. INTRODUCTION

Water is the medium for most naturally occurring reactions in biological systems,[1] and acts as a mixing agent for a number of organic molecules including alcohols. The OH group provides alcohols the ability to form hydrogen bonds making them compatible with water.[2] Interactions of such water−alcohol mixtures in porous systems change the structure and dynamics of the liquid phase within this matrix.[3] Pure liquids or liquid mixtures interact with the surface of the porous media through hydrogen bond interactions or hydrophobic and hydrophilic interactions. These interactions are, however, still poorly understood as they depend on the environment and the competition between surface−liquid interactions and liquid−liquid interactions. Understanding the effect of confinement and analyzing the structure and dynamics of the solvents may help in unraveling the water−alcohol interaction with surfaces at a molecular level. This can be the basis to optimize separation techniques for oil recovery and elimination of contamination or applications in lubrication.[4−6] Furthermore, water−alcohol mixtures in confinement have widespread applications in environmental studies[7,8] and biological investigations.[9,10] As a prominent example, 1-octanol[11−16] shows strong similarity to lipid molecules that encompass biological membranes, and is used as the model for membrane mimetics.[17,18] Since water and octanol are not miscible, the water−octanol partition coefficient is employed as a measure

to describe the partitioning of solutes between aqueous (hydrophilic) and organic (lipophilic) phases.[13,15,16] In particular, the water−octanol partition coefficient is universally used as a tool to predict the pharmacokinetic properties of drug molecules.[19−21]
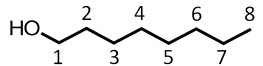
In the present paper, the combination of solid-state NMR spectroscopy and molecular dynamics (MD) simulations is employed to clarify the picture of water−octanol mixtures in confinement on the molecular scale. Solid-state NMR is a versatile technique for the determination of local structures and dynamics of small guest molecules in confined systems.[22−35] Cross-polarization magic angle spinning (CP-MAS)-based experiments provide direct structural information via analyzing heteronuclear dipolar interactions between nuclei in the mixtures and the confinement. In particular, CP-MAS heteronuclear correlation experiments (HETCOR) with frequency switched Lee−Goldburg homonuclear decoupling[36] (FSLG-HETCOR) allow us to estimate the strength of dipolar interactions, and thus, distances between protons and heteronuclei such as ^{29}Si or ^{13}C in a sample via variation of the contact time.[37−47] For example, ^{29}Si CP-MAS FSLG-HETCOR was recently employed to investigate water−iso-

Table 1. Liquid Employed for Wetting the SBA-15 + TSP Material

Alcohols	Liquids
1-octanol	neat 1-octanol (**1**)
	80:20 mol% mixture of 1-octanol and water (**2**)

butyric acid mixtures in confinement, and to shed more light on the microphase separation in this system[48] which was previously reported.[49,50] MD simulations yield the trajectories of all involved molecules, and thus, permit detailed insights into the structure and dynamics on short length and time scales. MD simulations have been applied to various aqueous mixtures confined in silica pores[48,51−54] as well as alumina pores[55] and have been proved to shed more light on the behavior of confined liquids.

Experimental studies[56−62] and MD simulations[52,53,55,63] have proposed that independent of the water content, water molecules show a strong preference to attach to the hydrophilic pore surface, and upon increasing the water−alcohol mole fractions they also occupy the pore center.

Although most of these studies have been focused on short chain alcohols, in the present work, we investigate 1-octanol as an example for long chain alcohols. We examine water−octanol mixtures in the mesoporous SBA-15 material[64] with solid-state NMR techniques to inspect the intermolecular interactions of these mixtures in confinement at room temperature. A prerequisite for the interpretation of the binary water−octanol system is the detailed knowledge of interaction of the individual constituents with the silica surface. For this reason, we performed a study on the adsorption of water and methanol on dried silica surfaces to reveal these interactions. Then, the structure and behavior of 1-octanol and water−1-octanol mixtures in the SBA-15 material are studied. Furthermore, we performed MD simulations of pure octanol and octanol−water mixtures at various mixing ratios and temperatures, evaluating concentrations, orientations, interaction energies, and hydrogen bonds as a function of the distance to the pore center.

2. EXPERIMENTAL SECTION

2.1. Synthesis of the Mesoporous SBA-15 Material. The mesoporous SBA-15 material was prepared according to the method of Zhao et al.[64] In a typical procedure, 7.46 g (0.026 equiv) of Pluronic 123 was dissolved in 324.5 mL deionized water. The mixture was then heated to 35 °C (308 K), and 9.05 mL of H_2SO_4 (96 wt %) was added. The solution was stirred for another 1 h, and 11.0 mL (1 equiv) of tetraethoxysilane was slowly added. After the addition was completed, the solution was stirred for 24 h at 35 °C (308 K). The resulting suspension was transferred into a Teflon bottle, and aged at 108 °C (381 K) for 40 h. The white precipitate was filtered off, washed with deionized water and acetone, and dried at 80 °C (353 K). The leftover template was removed by heating at 650 °C (923 K) for 24 h.

2.2. Characterization of the Mesoporous SBA-15 Material. The Brunauer−Emmett−Teller (BET) method was utilized to determine surface and pore parameters of the SBA-15 material. Adsorption−desorption measurements were carried out using the model Surfer by Thermo Fisher Scientific. The sample was dried for 2 days under vacuum using a turbomolecular pump (10^{-6} mbar) at 50 °C (323 K). Nitrogen gas was used for adsorption at the condensation point of

nitrogen. From the measurements (Figure S1a) a pore volume of 1.2 cm^3/g (Gurvich) and a specific surface area of 680 m^2/g (BET) was determined. The pore diameter was investigated by the Barrett, Joyner, and Halenda (BJH) method and was found to be 6.4 nm (Figure S1b).

2.3. Low Temperature ^{2}H-Solid-State-NMR Spectroscopy. *2.3.1. Sample Preparation.* Mobil Composition of Matter No. 41 (MCM-41, 65.28 mg) (d = 3.3 nm; S = 1040 m^2/g; V = 0.93 cm^3/g) was filled into an NMR sample tube. In the first step, the exchangeable silanol-protons were deuterated by repeated addition and removal of D_2O. Afterwards, the sample was dried and the remaining surface water molecules were removed by employing a vacuum of nominally 10^{-5} bar at a temperature of 200 °C for 2 days. Then 28 μL of methanol-d_4 were added under an argon atmosphere. Assuming cylindrical pores, this amount of methanol-d_4 corresponds to 46% of pore filling and is equivalent to the volume of a monolayer on the pore surface. After adding methanol, the sample was frozen in liquid nitrogen and then flame-sealed with a length of ca. 2 cm.

2.3.2. ^{2}H-Solid-State Measurements. All ^{2}H-solid-state spectra were measured with a laboratory-built ^{2}H-solid-state NMR spectrometer operating at 7 T. Since the spectrometer was previously described,[65] here only the salient experimental parameters are given. The probe was placed into an Oxford CF1200 dynamic Helium-flow cryostat system. The temperature was controlled via an Oxford ITC503 controller, attached to a Lakeshore Cernox CX-1010-1.4L sensor. Calibration of the sensor was performed via liquid nitrogen (−196 °C) and an ice−water mixture (0 °C). By employing this setup, the accuracy of the measured temperatures was found to be below ca. 0.07 K. A waiting period of one hour was employed before each measurement to allow for complete temperature equilibration of the sample. All spectra were measured in resonance with a solid echo sequence employing echo-delays between 30 and 40 μs and pulse-widths between 3.5 and 4.5 μs. Artifacts from pulse-imperfections were suppressed with a 16-pulse EXORCYCLE phase cycle.[66] Before Fourier transformation, the spectral data were phase-corrected by maximizing the echo amplitude, and the imaginary part of the echo was deleted to symmetrize the resulting powder spectra for the spectral deconvolution.

2.4. Room Temperature ^{1}H−^{29}Si CP-MAS and ^{1}H−^{29}Si FSLG-HETCOR NMR Experiments. *2.4.1. General.* 1-Octanol was purchased from Sigma-Aldrich (>99%) and used without any further purification. Deionized water was used in all experiments. Neat 1-octanol was obtained by placing 99% 1-octanol over activated 5 Å molecular sieve under argon in a glove box for 3−4 days. A mixture of 80:20 mol % of alcohol−water was chosen to obtain a single phase according to the phase diagram of octanol−water.[67]

2.4.2. Sample Preparation. SBA-15 (30 mg) was filled in a ZrO_2 rotor and the rotor was placed under vacuum overnight. The rotor was transferred to the glove box and closed with a Kel-F cap immediately. The rotor was placed in a spectrometer

Table 2. Lennard-Jones (LJ) Parameters for the 1-Octanol Sites[a]

sites/parameters	O	H_{OH}	C_{OH}	C_{H_3}	C_{H_2}	H_{CH_2}	H_{CH_3}
K_{cal}/mol	0.17	0	0.118	0.078	0.056	0.035	0.024
R_{min}/nm	3.446	2.0	4.383	4.080	4.020	2.680	2.680

[a]O and H_{OH} are the oxygen and hydrogen of the hydroxyl group, respectively. C_{OH} is the carbon linked to the hydroxyl group of 1-octanol, C_{H_3} and C_{H_2} are the carbons of the hydrocarbon chain, which are connected to three and two hydrogens, respectively. H_{CH_3} and H_{CH_2} are the hydrogens linked to C_{H_3} and C_{H_2}.

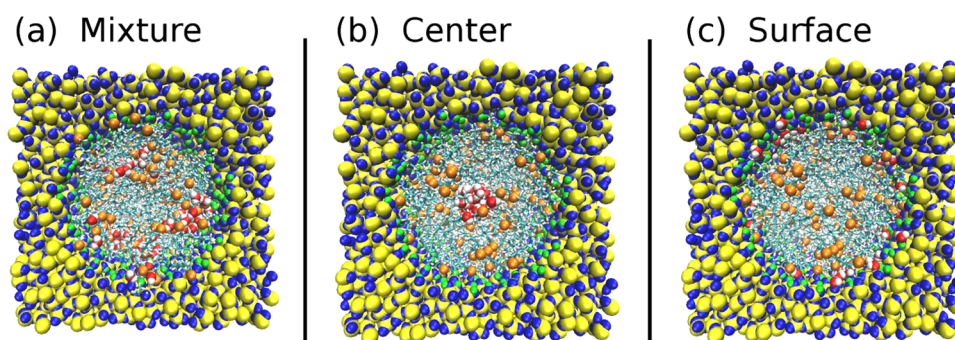**(a) Mixture   (b) Center   (c) Surface**

Figure 1. Snapshot of the starting configurations of the simulations of a mixture of 30 mol % water and 70 mol % 1-octanol in silica pore. (a) Initial configuration obtained from cutting a cylinder from the equilibrated mixture at 300 K (see Figure S2), (b, c) configurations for which water droplets are initially inserted in the pore center or near the pore surface, respectively. The yellow, blue, and green spheres are the silicon, oxygen, and hydrogen atoms of the silica pore, respectively. The red and white spheres are oxygen and hydrogen atoms of water molecules. The octanol oxygen atoms are represented as orange spheres.

and ^{1}H MAS and [29]Si CP-MAS spectra were measured. After the experiments, the rotor was transferred to the glove box and the cap was opened. Sodium 3-(trimethylsilyl)-2,2,3,3-tetradeuteropropionate (TSP, 6 mg) was added to the cavity formed by the centrifugation force during the spinning of the rotor. The rotor was placed in the spectrometer for measurements of dried SBA-15 with TSP. After measurements, the rotor was again transferred to the glove box, and 36 µL of the respective liquid (1, 2, see Table 1) was added to the sample using a pipette to reach approximately 80% pore filling (pore volume = 1.2 cm³/g). Note that a slightly larger amount of the liquid was used than required for an 80% filling because the sample contained TSP that adsorbs parts of the liquid. The rotor was kept for 15–20 min to allow the liquid to be adsorbed by the SBA-15 material.

2.4.3. [1]H–[29]Si CP-MAS and ^{1}H–^{29}Si FSLG-HETCOR NMR. All room temperature experiments were carried out on a Bruker AVANCE III HD spectrometer operating at 14 T corresponding to a frequency of 600.12 MHz for ^{1}H and 119.22 MHz for [29]Si. ZrO₂ (4 mm) rotors were used at a spinning rate of 8 kHz. [1]H–[29]Si CP-MAS and FSLG-HETCOR experiments were performed with a contact time of 3 ms. In addition, also longer contact times of 5, 7, or 9 ms, respectively, were utilized for recording the HETCOR spectra to observe long range correlations. For each spectrum 32 slices were acquired with 256 scans for each slice. A recycle delay of 4 s was utilized. Tppm15[68] decoupling was applied during data acquisition and FSLG homonuclear decoupling[36] was utilized with a decoupling field of 96 kHz during the evolution of the chemical shift. For referencing, TSP was added to the sample (6 mg TSP + 30 mg silica SBA-15). The [1]H–[29]Si FSLG-HETCOR spectra at room temperature were referenced internally with TSP (^{1}H and [29]Si signal was set to 0 ppm). The ^{1}H signal of TSP is used to scale the ^{1}H dimension of the 2D FSLG-HETCOR spectra.

3. SIMULATIONS SECTION

3.1. Simulation Details. MD simulations were performed with the NAMD simulation package.[66] Pure liquid 1-octanol was simulated using the CHARMM22[67] force field for hydrocarbon atom interactions, combined with the force field parameters of Debolt and Kollman[68] for the interaction with the hydroxyl group part. The density of the equilibrated 1-octanol system was found to be 0.8380 g/cm³, which is only 1.4% higher than the known experimental value for long chain alcohols.[17,69−71]

Two liquid mixtures containing 10 mol % of water (90 mol % of 1-octanol) molecules and 30 mol % of water (70 mol % of 1-octanol) molecules, respectively, were simulated using the simple point charge extended water model.[72] This model represents the water molecule by three point charges (0.4238e for hydrogen and −0.8476e for oxygen), and only the oxygen atom contains a van der Waals interaction potential.

Figure S2 shows that water and 1-octanol tend to demix for the 30 mol % mixture at normal pressure and room temperature. These mixtures were then inserted in a silica pore model provided by Geske and Vogel.[73] The atoms of 1-octanol and water were allowed to interact with silica atoms by means of a Coulomb and a Lennard-Jones (LJ) potential (see Table 2. The Gulmen−Thompson[74] model was used for the LJ parameters as well as for the partial charges assigned to each silica site. The hydrogen atoms of the hydroxyl groups were not kept fixed but restricted by the harmonic part of the angle potentials, as given by Hill and Sauer.[75] Interactions between the different atoms were dictated by the Lorentz−Berthelot mixing rules.[76,77]

All runs were carried out within the NPT ensemble for the bulk systems and the NVT ensemble for the mixtures in confinement. The covered temperature range was 300−425 K.

In the current investigation, only results obtained at 425 K are presented, where the system is well equilibrated. Effects on
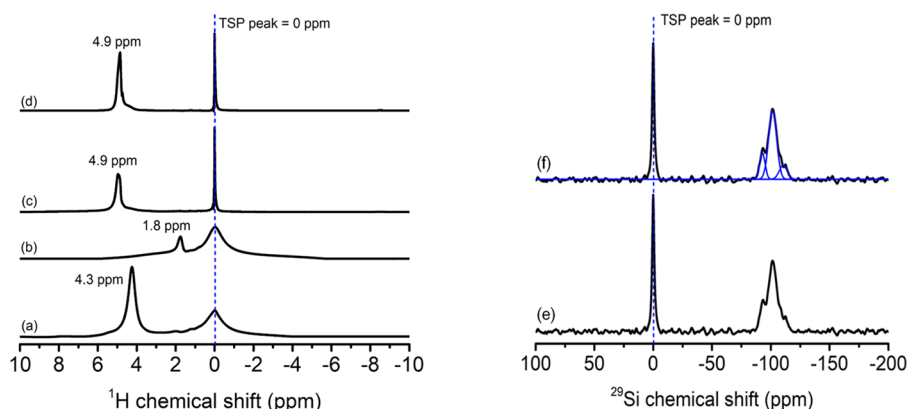
Figure 2. Normalized ^{1}H spectra of SBA-15 mixed with TSP measured at 8 kHz spinning at room temperature: (a) moist SBA-15, (b) dried SBA-15, (c) dried SBA-15 with one drop of water, and (d) dried SBA-15 with an additional drop of water. [1]H−[29]Si CP-MAS spectra of SBA-15 mixed with TSP measured at 8 kHz spinning nominally at room temperature: (e) moist SBA-15 and (f) deconvolution of spectrum (a).
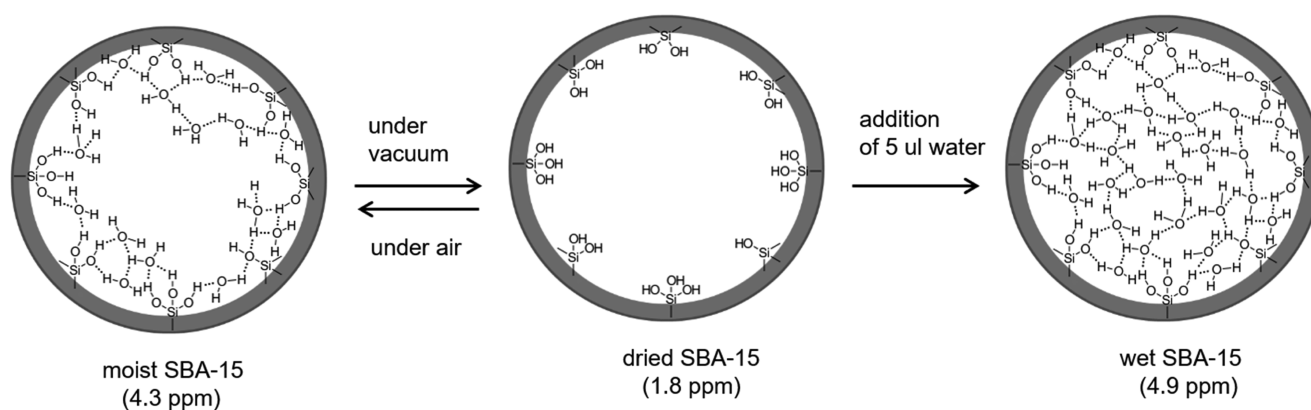

Figure 3. Schematic model of the wetting process of SBA-15.

the temperature are shown in the Supporting Information (Figure S3). A minimal equilibration time of 10−20 ns was used, which was required as the dynamics of molecules close to the pore surface get slow, and as water and 1-octanol tend to demix in the bulk. For simulations within the pore, a time step of 0.5 fs was used, simulations of the bulk were carried out with a time step of 1 fs. Periodic boundary conditions were applied, and the Coulomb interactions were evaluated using the particle mesh Ewald summation. A cut-off at 1.5 nm and a switching distance of 1.2 nm was used. In the NPT simulations, the pressure was kept at 1 bar using the Langevin−Piston method.[78] For the simulations in pore confinements, NVT simulations were performed using the Langevin thermostat,[79] with a coupling coefficient of 1.0 ps^{-1}, and with hydrogen atoms included in the Langevin dynamics. We checked the influence of the starting configuration by using three different starting configurations (Figure 1) of the confined mixture. First, the equilibrated bulk droplet is inserted inside the pore; second, water is initially inserted into the pore center and is surrounded by 1-octanol molecules; third, water is attached to the pore surface and the rest of the pore is filled with 1-octanol molecules.

4. RESULTS AND DISCUSSION

4.1. Silica SBA-15 with Water. In the first step, the behavior of water in the SBA-15 material was revisited by solid-state NMR because these results are required to understand the behavior of alcohols or alcohol mixtures in confinement.

The SBA-15 material is hydrophilic as it contains large amounts of surface −OH groups attached to Si atoms, which enable the formation of hydrogen bonds.[80,81] Thus, water molecules present in air may be easily adsorbed as previously shown by ^{1}H MAS studies by some of us.[1]

The effect of water interaction on the SBA-15 material is illustrated in the ^{1}H MAS spectra of SBA-15 mixed with TSP (Figure 2). In Figure 2a, the proton spectrum of SBA-15, which was stored in air (moist SBA-15), is shown. One signal is obtained at 4.3 ppm, which is attributed to surface Si−OH protons that interact with water molecules, and a second broad one at 0 ppm which is assigned to TSP. When the same rotor was kept under vacuum overnight (dried SBA-15), and the proton spectrum was measured (Figure 2b), the signal at 4.3 ppm shifted to 1.8 ppm, which is in agreement with the proton signal for dried silica.[1] After the addition of 5 μL of water to this sample (wet SBA-15) (Figure 2c), the signal shifted from 1.8 to 4.9 ppm. Additionally, a decrease in the line width of the TSP signal is observed, which most probably refers to dissolution of TSP when adding water to the sample. Further addition of 5 μL water to this sample (Figure 2d) yielded no significant shift of the signal at 4.9 ppm, but the intensity of the signal enhanced, which is in agreement with the increased number of H_2O molecules in this sample.

The process of wetting is illustrated in Figure 3. In air, the SBA-15 material adsorbs water, which covers a monolayer of water molecules interacting with the surface via hydrogen bonds (moist SBA-15). The water molecules are desorbed

under vacuum and only the free silanol groups remain on the surface (dried SBA-15). Upon addition of water to the dried SBA-15 material pore filling occurred, where next to a monolayer, multilayers of H_2O molecules are also formed (wet SBA-15). This formation of multilayers may explain the differences in chemical shifts between moist SBA-15 (4.3 ppm) and wet SBA-15 (4.9 ppm).

Next to the ^1H MAS spectra, the ^{29}Si CP-MAS spectra of moist, dried, and wet SBA-15 were recorded. Since all spectra showed the same line-shape, an exemplary ^{29}Si CP-MAS spectrum of moist SBA-15 recorded with 3 ms contact time is displayed in Figure 2e,f. The signal at 0 ppm corresponds to TSP, which was employed as the internal reference. Furthermore, three distinguishable signals are observed, which are clearly assigned to the surface Q_2 (−93.0 ppm) and Q_3 (−101.5 ppm) groups, as well as Q_4 (−112.0 ppm) groups from the bulk silica material.[82]

4.2. Silica MCM-41 with Methanol. Typical desorption of non-covalently bound alcohols on silica occurs at temperatures of ca. 80−120 °C as shown by Björklund in thermogravimetric analysis measurements.[83] However, below this temperature thermally activated surface hopping or liquid surface exchange processes are in principle feasible. They correspond to the breaking and re-establishment of hydrogen bonds. For the determination of the binding interaction of an alcohol to the silica surface, deuterated methanol as the smallest alcohol was employed inside MCM-41, since the latter has in general a better-defined surface.[27]

Figure 4 shows the ^2H NMR spectra of methanol-d_4 in MCM-41, measured at four different temperatures. At 160 K,
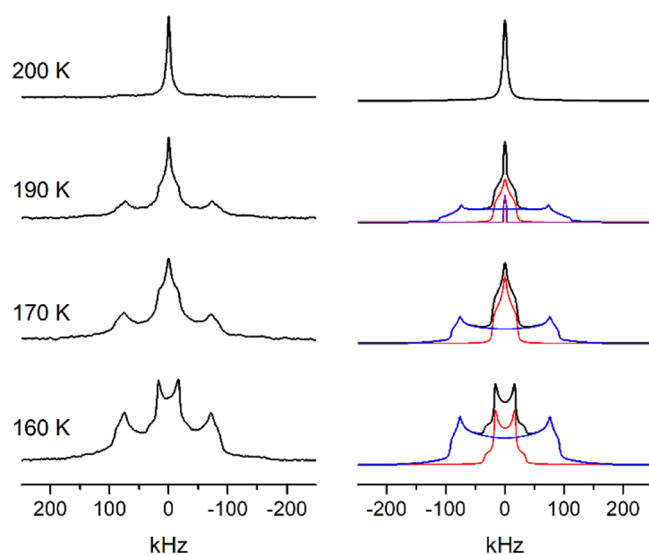

Figure 4. Experimental (left) and simulated ^2H NMR spectra of methanol-d_4 in MCM-41. The simulation of the low temperature spectra shows a deconvolution into −OD (blue), −CD$_3$ (red), and liquid like (magenta) components.

the spectrum is a superposition of a broad component with Q_{zz} = 169 kHz and a narrower component with Q_{zz} = 35 kHz. Both spectra exhibit pronounced singularities. While the first value is indicative for a rigid −OD signal, the second value is slightly below the value of a typical −CD$_3$ group (42 kHz), performing fast rotations around the C$_3$-axis.[84,85] Thus, the broad signal stems from the hydroxyl groups of the silica and the methanol and the narrower signal from the methyl groups

of the methanol. In contrast to the signal of the −CD$_3$, which corresponds to an axial symmetric tensor ($\eta \approx 0$), the signals attributed to the −OD group show some asymmetry of the tensor ($\eta \approx 0.1$). The reduction of the quadrupolar interaction of the methyl group is an indication of motions of the −C−O vector of the methanol molecules on the surface, which cause a partial averaging of the −CD$_3$ quadrupolar interaction.

In the spectrum measured at 170 K, there are again both contributions as in the previous spectra, but there is a substantial change in the center, where the asymmetry of the methyl group has changed from an ($\eta \approx 0$) to an ($\eta \approx 1$) spectrum. This change could either be the result of the onset of an anisotropic motion of the methanol molecules, such as an asymmetric vibration or wobbling or a superposition of the spectra of bound methanol and methanol molecules, exhibiting relatively slow isotropic motions, for example in the form of a surface hopping between different silanol groups, similar to pyridine.[27] Upon further increase of the temperature to 190 K, the intensities of the bound methanol-signals have strongly decreased and a narrow isotropic peak has appeared in the center of the spectrum, which at 200 K completely dominates the spectrum, showing that at this temperature the spectrum is dominated by free moving methanol molecules. These spectra clearly show that above 190 K the rate of formation and breakage of hydrogen bonds is sufficiently fast, resulting in full averaging of the quadrupolar interaction.

4.3. SBA-15 with 1-Octanol. Figure 5a,b shows the room temperature ^1H−^{29}Si CP-MAS FSLG-HETCOR spectra of dried SBA-15 + TSP mixed with 1-octanol (1), measured with contact times of 3 and 9 ms, respectively. The filling factor of 1-octanol in this sample was approximately 80% of the pore volume of silica. The spectrum in Figure 5a shows a signal at 4.9 ppm similar to the proton signal obtained for the water-saturated SBA-15 material (Figure 2c) (Si−OH···OH$_2$).

Though, the 1-octanol was dried over a molecular sieve and the SBA-15 material was dried under vacuum, the absence of water within the system may not be guaranteed. As seen in Figure 5b, the "iced water" signal is present around 8 ppm, indicating water content, despite the drying process.

This signal is not related to the protonated TSP, since an additional tiny signal at 6−7 ppm is also visible in the spectrum of the moist SBA material (see Supporting Information Figure S4a). According to ref 86, this signal may be related to strongly bound water (iced water).

Therefore, this peak may be interpreted as a fingerprint of the water content or as a signal from the OH group of the octanol interacting with the iced water via chemical exchange of protons. Although the data obtained from the experiments on methanol in MCM clearly demonstrate the breakage of hydrogen bridges of the methanol−MCM system at 200 K sufficiently fast to average all quadrupole interactions, it is reasonable to assume that at room temperature (RT) the breakage will be sufficiently fast to allow these exchange processes.

The resulting chemical shift under sufficiently fast exchange may be estimated[62] by averaging the chemical shift of the OH−1-octanol group in an exchange free environment, i.e., 1-octanol in CDCl$_3$, 1.4 ppm with the chemical shift of the iced water at 8 ppm, yielding 4.7 ppm, which is reasonably close to the observed value of 4.9 ppm.

If this assumption holds true, i.e., the high breakage rate of the hydrogen bridges, 1-octanol molecules may be present in the system but not involved in exchange processes and not
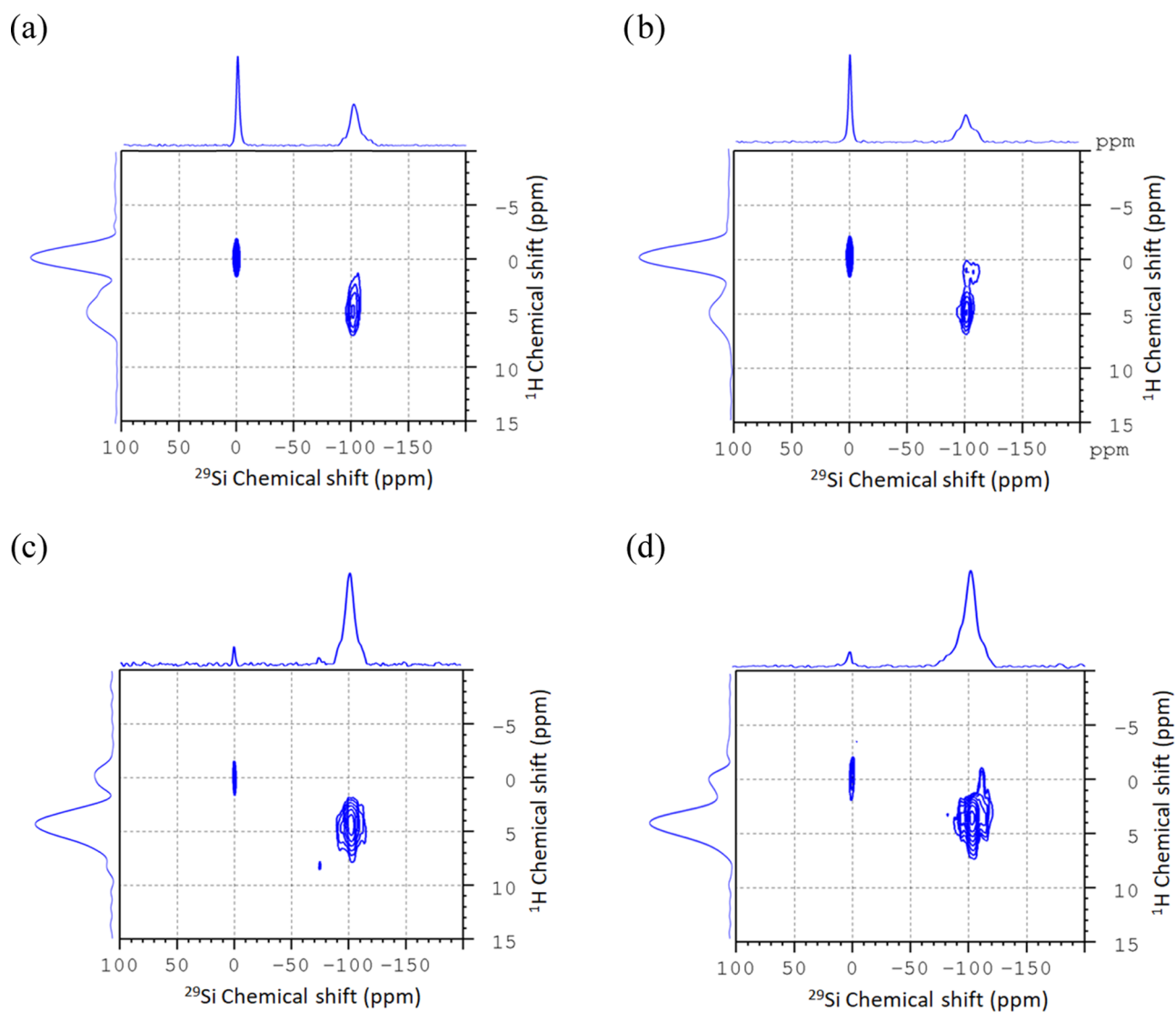
Figure 5. Room temperature $^1H-^{29}Si$ CP-MAS FSLG-HETCOR experiment measured at 8 kHz spinning. (a, b) Dried SBA-15 mixed with neat 1-octanol measured with a contact time of (a) 3 ms and (b) 9 ms. (c, d) Dried SBA-15 + TSP mixed with a mixture of 80:20 mol % of 1-octanol and water with a contact time of (c) 3 ms and (d) 9 ms.
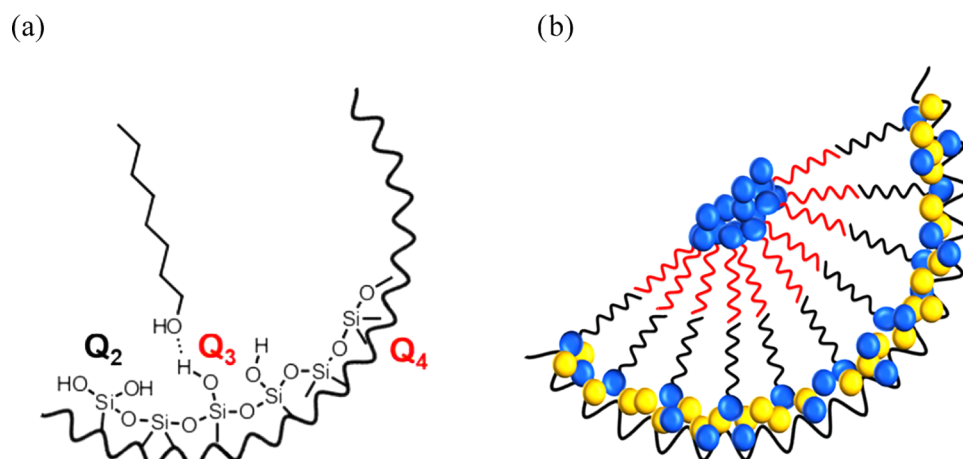

Figure 6. (a) Models for interactions of the pore surface of SBA-15 with 1-octanol. (b) Model depicting the feasible bilayer formation of 1-octanol inside the pore. Water molecules are concentrated near the pore wall as well as in the pore center. The intermediated area between the pore wall and the pore center is occupied by the aliphatic hydrophobic chains of the 1-octanol molecules.
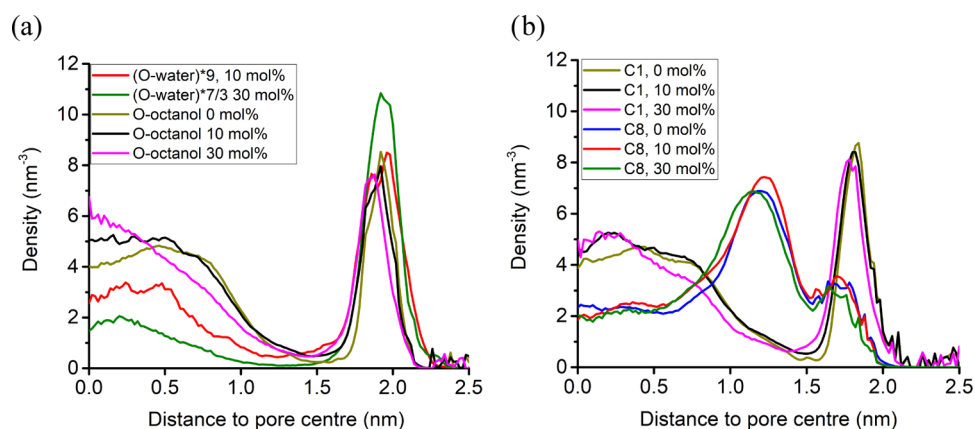
Figure 7. Number density profile of (a) oxygens of water and 1-octanol molecules and (b) of carbons (first carbon C1 and last carbon of chain C8) of 1-octanol molecules, for 0, 10, and 30 mol % water. The density of water molecules is multiplied by the indicated factor for a better comparison. These data correspond to a simulation at 425 K.
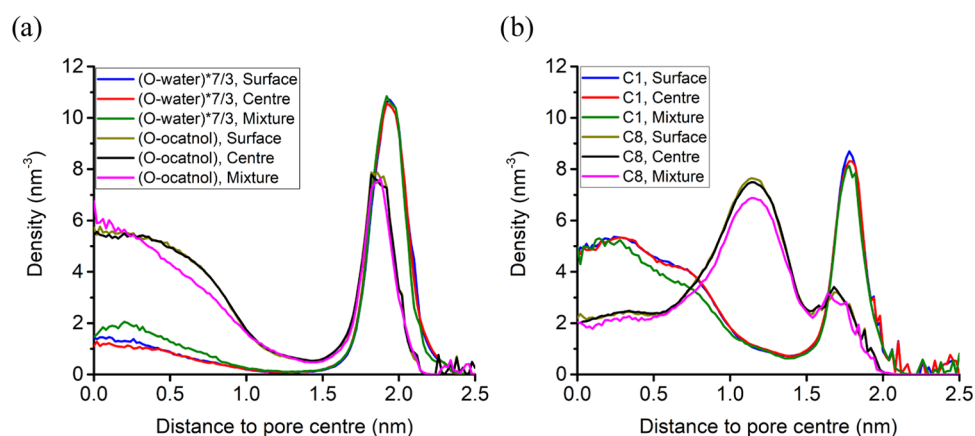

Figure 8. Number density profile for 30 mol % water molecules at 425 K of (a) the oxygens of water and octanol molecules, and (b) the carbons (first carbon (C1) and last carbon (C8) of the chain) of 1-octanol molecules, for the surface, center, and mixture starting configuration. The density of water molecules is multiplied by the indicated factor 7:3 for a better comparison.

bound via hydrogen bridges to the surface. These molecules may be expected to be mobile and far from the surface, that is, will be seen in FSLG-HETCOR experiments conducted with long contact times.

To test this assumption, the FSLG-HETCOR experiment was repeated with a contact time of 9 ms (Figure 5b). Interestingly, an additional signal in the ^{1}H dimension at ca. 1 ppm appeared, which correlates with the Q_3 and Q_4 groups in the ^{29}Si dimension, remarkably with a higher intensity on the Q_4-groups. The higher intensity on the Q_4-groups implies significantly higher probability of finding the 1-octanol molecule in a water poor environment near Q_4-groups. By taking into account the roughness of the SBA surface, iced water free cavities may be present. 1-Octanol molecules in the vicinity of such a cavity possess exchangable free OH protons. Since the correlations on Q_3 groups stems mainly from ^{29}Si located at "flat" parts of the SBA surface, the probability of finding iced water free flat parts weights the correlation intensities. Therefore, by adding water to the system, the correlation on the Q_3 groups is expected to disappear, whereas the correlations on the Q_4 groups should remain.

The corresponding experiments on the 80:20 mol % of 1-octanol and water mixture sample (Figure 5c,d) do not show the Q_3 group correlation, indeed. One may argue at this point that this correlation may be due to an interaction of single

water molecules or TSP with the silica surface. However, we carefully repeated the experiments on samples containing either only water, only TSP, or TSP–water mixtures. The peak around 1 ppm never appeared in the FSLG-HETCOR experiments when the 1-octanol content is zero.

From these experimental results, the model displayed in Figure 6a can be derived. This model illustrates that the polar OH groups of 1-octanol are in close contact with the surface and interact via hydrogen bonds/chemical exchange, while the non-polar aliphatic group avoids the contact with the hydrophilic silica surface. This demonstrates that hydrophilic–hydrophilic interactions dominate, due to strong hydrogen bonding, compared to weak hydrophilic–hydrophobic interactions in the system.

4.4. Molecular Dynamic Simulations. Figure 7a displays the number density profile of oxygen atoms of water and 1-octanol, showing that oxygen atoms of water and 1-octanol are concentrated near the pore wall as well as in the pore center. The density distributions of the first (C1) and the last (C8) carbon of the 1-octanol chain, plotted in Figure 7b, display a similar tendency. C1 is concentrated near the pore wall as well as in the pore center, whereas C8 shows a peak roughly in the intermediate pore region. For the carbons C2–C7, the overall density profiles are given in Figure S5 and show the maximum concentration in the range between the wall and the
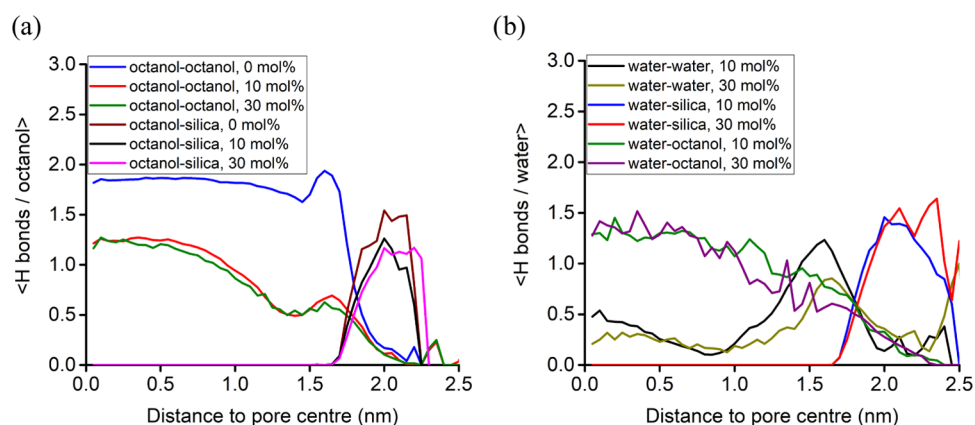
Figure 9. (a) Profile of the number of hydrogen bonds per octanol molecule shared with octanol molecules (octanol−octanol) and silanol groups (octanol−silica). (b) The equivalent profile for water, including the hydrogen bonds between water molecules (water−water), water and silanol groups (water−silica), and water and octanol molecules (water−octanol).

intermediate pore region. A comparison of the C1 and C8 density distributions in systems containing 0, 10, and 30 mol % water, reveals that they are not significantly affected by the inclusion of water. With increasing water content, water molecules accumulate somewhat closer to the pore center and near the pore surface. This is not very surprising since the tendency of water molecules is to stay close to the hydrophilic centers of 1-octanol or at the silica surface.

To confirm the latter, we performed a simulation with only water and no 1-octanol in the pore at 15% pore filling. In Figure S6, it is shown that water molecules prefer to stay near the pore wall.[87] Furthermore, from Figures 7 and S5 a bilayer formation is assumed, as the length of the 1-octanol molecule is roughly 0.9 nm. Therefore, two layers of 1-octanol molecules that interact via their hydrophobic aliphatic chains may arrange inside the pore as illustrated schematically in Figure 6b.

In the following step, we checked whether the obtained distribution depends on the starting configuration of the water−octanol mixture. Several simulations were performed with the starting configurations shown in Figure 1. The "center" is defined as the configuration in which the water droplet is initially in the pore center, whereas the "surface" is defined as the configuration where water is initially placed near the pore surface. The "mixture" starting configuration is obtained by inserting an equilibrated droplet of the octanol−water bulk mixture into the pore. This droplet was obtained by cutting a cylinder from the equilibrated bulk mixture as shown in Figure S2. The resulting density profiles are displayed in Figure 8 and show that the number of oxygens or carbons aggregating near the pore wall does not depend on the starting configuration. Although, the same trend is seen in the intermediate pore region, in the center of the pore small fluctuations are noticeable for the mixture starting configuration. This may be related to the fact that in the mixture starting configuration, some water and 1-octanol molecules are initially hydrogen-bonded, and thus leads to bigger fluctuations when the energy is minimized for the system to reach the equilibrated distribution. However, these are tiny fluctuations as one can also see in the energy plot in Figure S7b. The water−silica energy decreases for the center and mixture starting configuration, and it slightly increases for the surface starting configuration, until reaching the balanced energy. In a similar manner, the water−water energy increases for the center as well as for the mixture starting configuration, whereas

for the surface starting configuration the energy at equilibrium is almost reached for very short simulation times.

To better understand these observations, we evaluated the average number of hydrogen bonds per octanol molecule and per water molecule, as shown in Figure 9, inside the pore for different water−1-octanol ratios, since they play a decisive role in determining the configuration of lowest energy. We defined two molecules to be connected via a hydrogen bond if the O···O separation is less than 0.335 nm and the angle between the intramolecular O−H vector and the intermolecular O···O vector is less than 30°.

First, it is observed that the average number of hydrogen bonds per octanol molecule shared with octanol molecules (octanol−octanol) (Figure 9a) in the pore diminishes when water is added. This is expected because some of the octanol molecules form hydrogen bonds with water molecules. The average number of hydrogen bonds per octanol molecule shared with surface silanol groups (octanol−silica) decreases slightly with the increasing water content (Figure 9a), whereas the average number of hydrogen bonds per water molecule shared with surface silanol groups (water−silica) increases with the water content (Figure 9b). This is understandable because silica favors to form H-bonds with water compared to octanol due to its hydrophilicity. This trend is in agreement with the observation made in Figure 7a that the amount of water molecules increases near the pore surface and reduces near the pore center with a higher water−octanol ratio.

The average number of hydrogen bonds shared between water and octanol molecules (water−octanol) is nearly independent of the mixing percentage as shown in Figure 9b.

Approximately 1.5 hydrogen bonds per octanol (and per water) molecule are formed with the silica surface, which suggests that the electrostatic energy between octanol and surface molecules is comparable to the one between water and surface molecules. This observation is confirmed by the evaluated electrostatic energy (Figure S8b), where the energy between water and silica almost converges to the same value as the energy between octanol and silica. Fluctuations in the H-bond profiles near the pore surface (Figure 9) are attributed to the presence of very few octanol molecules in the silica wall, which influences the calculation of the average number of the hydrogen bonds in silica walls.

4.5. Comparison of Solid-State NMR and MD Simulation Data. Both, NMR experimental results and MD

simulation results clearly demonstrate that the hydroxyl groups from water and octanol tend to be located near the pore surface and form hydrogen bonds with the hydrophilic sites of the silica surface. Along with this, octanol and water also form hydrogen bonds with each other as shown by MD simulations.

While the NMR study clearly reveals the orientation and interaction of octanol−water in the pore surface region, MD simulations also shed light on orientations and interactions in the pore center region along with the pore surface region. Deuterium NMR experiments of methanol-d_4 have shown that alcohols can be mobile on the silica at temperatures above ca. 190 K. Such a mobility was also observed in the RT-simulations of 1-octanol molecules adsorbed on the silica surface.

MD simulations suggest the formation of a bilayer-like structure inside the pore (4 nm) with hydroxyl groups oriented to the pore surface and in the pore center, and the hydrocarbon chain in the pore intermediate region. This possibility to form bilayer-like structures is also indicated by NMR studies, which suggest an alignment of octanol molecules. Nevertheless, the dipolar interaction of the protons in the second octanol layer with the silica surface is too weak to be detected. In summary, the combination of solid-state NMR and MD simulations is necessary to get a clear picture on the structure of octanol−water mixtures in the confined environment of mesoporous materials.

5. CONCLUSIONS

Solid-state NMR investigations and MD simulations revealed the orientation and interaction of octanol−H_2O confined in mesoporous silica. These studies show that the hydroxyl groups of octanol and water stay near the pore surface through hydrogen bonds with silica sites, while the hydrocarbon chains are located in the range between the surface and the center. The orientation seems to be nearly independent from the ratio between water and octanol molecules in our simulations (0−30 mol % of water). However, the mixing ratio significantly influences the formation of hydrogen bonds between octanol−octanol and octanol−silica. With increasing water content, water replaces the octanol, and thus, silica and octanol prefer to form hydrogen bonds with water instead of octanol. Finally, we wish to note that further insights about the chain mobility of 1-octanol can be obtained by ^1H T_2' measurements or ^2H NMR measurements of selectively deuterated isotopomers.

■ ASSOCIATED CONTENT

ⓢ Supporting Information

The Supporting Information is available free of charge on the ACS Publications website at DOI: 10.1021/acs.jpcc.8b04745.

Nitrogen adsorption data; simulation snapshots of final configuration; calculated density profiles of different oxygen and carbon atoms; additional room temperature $^1H-^{29}Si$ CP-MAS FSLG-HETCOR spectra; calculated energy time curves (PDF)

■ AUTHOR INFORMATION

Corresponding Authors
*E-mail: drossel@fkp.tu-darmstadt.de (B.D.).
*E-mail: gutmann@chemie.tu-darmstadt.de (T.G.).
*E-mail: gerd.buntkowsky@chemie.tu-darmstadt.de (G.B.).

ORCID Ⓘ

Torsten Gutmann: 0000-0001-6214-2272

Gerd Buntkowsky: 0000-0003-1304-9762

Notes

The authors declare no competing financial interest.

■ ACKNOWLEDGMENTS

■ REFERENCES

(1) Grünberg, B.; Emmler, T.; Gedat, E.; Shenderovich, I.; Findenegg, G. H.; Limbach, H.-H.; Buntkowsky, G. Hydrogen Bonding of Water Confined in Mesoporous Silica Mcm-41 and Sba-15 Studied by 1H Solid-State NMR. *Chem. - Eur. J.* **2004**, *10*, 5689−5696.

(2) Hu, K.; Zhou, Y.; Shen, J.; Ji, Z.; Cheng, G. Microheterogeneous Structure of 1-Octanol in Neat and Water-Saturated State. *J. Phys. Chem. B* **2007**, *111*, 10160−10165.

(3) Gelb, L. D.; Gubbins, K. E. Studies of Binary Liquid Mixtures in Cylindrical Pores: Phase Separation, Wetting and Finite-Size Effects from Monte Carlo Simulations. *Phys. A* **1997**, *244*, 112−123.

(4) Góźdź, W. T.; Gubbins, K. E.; Panagiotopoulos, A. Z. Liquid-Liquid Phase Transitions in Pores. *Mol. Phys.* **1995**, *84*, 825−834.

(5) Sliwinska-Bartkowiak, M.; Sikorski, R.; Sowers, S. L.; Gelb, L. D.; Gubbins, K. E. Phase Separations for Mixtures in Well-Characterized Porous Materials: Liquid-Liquid Transitions. *Fluid Phase Equilib.* **1997**, *136*, 93−109.

(6) Sliwinska-Bartkowiak, M.; Sowers, S. L.; Gubbins, K. E. Liquid-Liquid Phase Equilibria in Porous Materials. *Langmuir* **1997**, *13*, 1182−1188.

(7) Brown, G. E., Jr. Surface Science: How Minerals React with Water. *Science* **2001**, *294*, 67−69.

(8) Leo, A.; Hansch, C.; Elkins, D. Partition Coefficients and Their Uses. *Chem. Rev.* **1971**, *71*, 525−616.

(9) Ball, P. Water as an Active Constituent in Cell Biology. *Chem. Rev.* **2008**, *108*, 74−108.

(10) Prime, K. L.; Whitesides, G. M. Self-Assembled Organic Monolayers: Model Systems for Studying Adsorption of Proteins at Surfaces. *Science* **1991**, *252*, 1164−1167.

(11) Best, S. A.; Merz, K. M.; Reynolds, C. H. Free Energy Perturbation Study of Octanol/Water Partition Coefficients: Comparison with Continuum Gb/Sa Calculations. *J. Phys. Chem. B* **1999**, *103*, 714−726.

(12) Bolts, J. M.; Wrighton, M. S. Correlation of Photocurrent-Voltage Curves with Flat-Band Potential for Stable Photoelectrodes for the Photoelectrolysis of Water. *J. Phys. Chem.* **1976**, *80*, 2641−2645.

(13) Chen, B.; Siepmann, J. I. Partitioning of Alkane and Alcohol Solutes between Water and (Dry or Wet) 1-Octanol. *J. Am. Chem. Soc.* **2000**, *122*, 6464−6467.

(14) Chen, B.; Siepmann, J. I. Microscopic Structure and Solvation in Dry and Wet Octanol. *J. Phys. Chem. B* **2006**, *110*, 3555−3563.

(15) Garrido, N. M.; Queimada, A. J.; Jorge, M.; Macedo, E. A.; Economou, I. G. 1-Octanol/Water Partition Coefficients of N-Alkanes from Molecular Simulations of Absolute Solvation Free Energies. *J. Chem. Theory Comput.* **2009**, *5*, 2436−2446.

(16) Lyubartsev, A. P.; Jacobsson, S. P.; Sundholm, G.; Laaksonen, A. Solubility of Organic Compounds in Water/Octanol Systems. A Expanded Ensemble Molecular Dynamics Simulation Study of Log P Parameters. *J. Phys. Chem. B* **2001**, *105*, 7775−7782.

(17) MacCallum, J. L.; Tieleman, D. P. Structures of Neat and Hydrated 1-Octanol from Computer Simulations. *J. Am. Chem. Soc.* **2002**, *124*, 15085−15093.

(18) Sassi, P.; Paolantoni, M.; Cataliotti, R. S.; Palombo, F.; Morresi, A. Water/Alcohol Mixtures: A Spectroscopic Study of the Water-

Saturated 1-Octanol Solution. *J. Phys. Chem. B* **2004**, *108*, 19557−19565.

(19) Hansch, C.; Björkroth, J. P.; Leo, A. Hydrophobicity and Central Nervous System Agents: On the Principle of Minimal Hydrophobicity in Drug Design. *J. Pharm. Sci.* **1987**, *76*, 663−687.

(20) Martinez, M. N.; Amidon, G. L. A Mechanistic Approach to Understanding the Factors Affecting Drug Absorption: A Review of Fundamentals. *J. Clin. Pharmacol.* **2002**, *42*, 620−643.

(21) Smith, R. N.; Hansch, C.; Ames, M. M. Selection of a Reference Partitioning System for Drug Design Work. *J. Pharm. Sci.* **1975**, *64*, 599−606.

(22) Vyalikh, A.; Emmler, T.; Gedat, E.; Shenderovich, I.; Findenegg, G. H.; Limbach, H. H.; Buntkowsky, G. Evidence of Microphase Separation in Controlled Pore Glasses. *Solid State Nucl. Magn. Reson.* **2005**, *28*, 117−124.

(23) Vyalikh, A.; Emmler, T.; Grunberg, B.; Xu, Y.; Shenderovich, I.; Findenegg, G. H.; Limbach, H. H.; Buntkowsky, G. Hydrogen Bonding of Water Confined in Controlled-Pore Glass 10−75 Studied by H-1-Solid State NMR. *Z. Phys. Chem.* **2007**, *221*, 155−168.

(24) Vyalikh, A.; Emmler, T.; Shenderovich, I.; Zeng, Y.; Findenegg, G. H.; Buntkowsky, G. ^{2}H-Solid State NMR and DSC Study of Isobutyric Acid in Mesoporous Silica Materials. *Phys. Chem. Chem. Phys.* **2007**, *9*, 2249−2257.

(25) Gedat, E.; Schreiber, A.; Findenegg, G.; Shenderovich, I.; Limbach, H. H.; Buntkowsky, G. Stray Field Gradient NMR Reveals Effects of Hydrogen Bonding on Diffusion Coefficients of Pyridine in Mesoporous Silica. *Magn. Reson. Chem.* **2001**, *39*, S149−S157.

(26) Gedat, E.; Schreiber, A.; Albrecht, J.; Emmler, T.; Shenderovich, I.; Findenegg, G. H.; Limbach, H. H.; Buntkowsky, G. 2h Solid State NMR Study of Benzene-D6 Confined in Mesoporous Silica SBA-15. *J. Phys. Chem. B* **2002**, *106*, 1977−1984.

(27) Shenderovich, I.; Buntkowsky, G.; Schreiber, A.; Gedat, E.; Sharif, S.; Albrecht, J.; Golubev, N. S.; Findenegg, G. H.; Limbach, H. H. Pyridine-N-15 - a Mobile NMR Sensor for Surface Acidity and Surface Defects of Mesoporous Silica. *J. Phys. Chem. B* **2003**, *107*, 11924−11939.

(28) Dosseh, G.; Xia, Y.; Alba-Simionesco, C. Cyclohexane and Benzene Confined in MCM-41 and SBA-15: Confinement Effects on Freezing and Melting. *J. Phys. Chem. B* **2003**, *107*, 6445−6453.

(29) Lusceac, S. A.; Koplin, C.; Medick, P.; Vogel, M.; Brodie-Linder, N.; LeQuellec, C.; Alba-Simionesco, C.; Rössler, E. A. Type a Versus Type B Glass Formers: NMR Relaxation in Bulk and Confining Geometry. *J. Phys. Chem. B* **2004**, *108*, 16601−16605.

(30) Alba-Simionesco, C.; Coasne, B.; Dosseh, G.; Dudziak, G.; Gubbins, K. E.; Radhakrishnan, R.; Sliwinska-Bartkowiak, M. Effects of Confinement on Freezing and Melting. *J. Phys.: Condens. Matter* **2006**, *18*, R15−R68.

(31) Buntkowsky, G.; Breitzke, H.; Adamczyk, A.; Roelofs, F.; Emmler, T.; Gedat, E.; Grünberg, B.; Xu, Y.; Limbach, H.-H.; Shenderovich, I.; Vyalikh, A.; Findenegg, G. Structural and Dynamical Properties of Guest Molecules Confined in Mesoporous Silica Materials Revealed by NMR. *Phys. Chem. Chem. Phys.* **2007**, *9*, 4843−4853.

(32) Findenegg, G. H.; Jähnert, S.; Akcakayiran, D.; Schreiber, A. Freezing and Melting of Water Confined in Silica Nanopores. *ChemPhysChem* **2008**, *9*, 2651−2659.

(33) Geppi, M.; Borsacchi, S.; Mollica, G.; Veracini, C. A. Applications of Solid-State NMR to the Study of Organic/Inorganic Multicomponent Materials. *Appl. Spectrosc. Rev.* **2008**, *44*, 1−89.

(34) Vogel, M. NMR Studies on Simple Liquids in Confinement. *Eur. Phys. J.: Spec. Top.* **2010**, *189*, 47−64.

(35) Werner, M.; Rothermel, N.; Breitzke, H.; Gutmann, T.; Buntkowsky, G. Recent Advances in Solid State NMR of Small Molecules in Confinement. *Isr. J. Chem.* **2014**, *54*, 60−73.

(36) van Rossum, B. J.; Förster, H.; de Groot, H. J. M. High-Field and High-Speed Cp-MAS C-13 NMR Heteronuclear Dipolar-Correlation Spectroscopy of Solids with Frequency-Switched Lee-Goldburg Homonuclear Decoupling. *J. Magn. Reson.* **1997**, *124*, 516−519.

(37) van Rossum, B. J.; de Groot, C. P.; Ladizhansky, V.; Vega, S.; de Groot, H. J. M. A Method for Measuring Heteronuclear (^{1}H-^{13}C) Distances in High Speed MAS NMR. *J. Am. Chem. Soc.* **2000**, *122*, 3465−3472.

(38) Trebosc, J.; Wiench, J. W.; Huh, S.; Lin, V. S. Y.; Pruski, M. Studies of Organically Functionalized Mesoporous Silicas Using Heteronuclear Solid-State Correlation NMR Spectroscopy under Fast Magic Angle Spinning. *J. Am. Chem. Soc.* **2005**, *127*, 7587−7593.

(39) Paul, G.; Steuernagel, S.; Koller, H. Non-Covalent Interactions of a Drug Molecule Encapsulated in a Hybrid Silica Gel. *Chem. Commun.* **2007**, 5194−5196.

(40) Wiench, J. W.; Avadhut, Y. S.; Maity, N.; Bhaduri, S.; Lahiri, G. K.; Pruski, M.; Ganapathy, S. Characterization of Covalent Linkages in Organically Functionalized MCM-41 Mesoporous Materials by Solid-State NMR and Theoretical Calculations. *J. Phys. Chem. B* **2007**, *111*, 3877−3885.

(41) Ben Shir, I.; Kababya, S.; Schmidt, A. Binding Specificity of Amino Acids to Amorphous Silica Surfaces: Solid-State NMR of Glycine on SBA-15. *J. Phys. Chem. C* **2012**, *116*, 9691−9702.

(42) Kobayashi, T.; Mao, K.; Wang, S. G.; Lin, V. S.; Pruski, M. Molecular Ordering of Mixed Surfactants in Mesoporous Silicas: A Solid-State NMR Study. *Solid State Nucl. Magn. Reson.* **2011**, *39*, 65−71.

(43) Rapp, J. L.; Huang, Y. L.; Natella, M.; Cai, Y.; Lin, V. S. Y.; Pruski, M. A Solid-State NMR Investigation of the Structure of Mesoporous Silica Nanoparticle Supported Rhodium Catalysts. *Solid State Nucl. Magn. Reson.* **2009**, *35*, 82−86.

(44) Nayeri, M.; Aronson, M. T.; Bernin, D.; Chmelka, B. F.; Martinelli, A. Surface Effects on the Structure and Mobility of the Ionic Liquid C6c1imtfsi in Silica Gels. *Soft Matter* **2014**, *10*, 5618−5627.

(45) Ukmar, T.; Cendak, T.; Mazaj, M.; Kaucic, V.; Mali, G. Structural and Dynamical Properties of Indomethacin Molecules Embedded within the Mesopores of SBA-15: A Solid-State NMR View. *J. Phys. Chem. C* **2012**, *116*, 2662−2671.

(46) Werner, M.; Rothermel, N.; Breitzke, H.; Gutmann, T.; Buntkowsky, G. Recent Advances in Solid State NMR of Small Molecules in Confinement. *Isr. J. Chem.* **2014**, *54*, 60−73.

(47) Gutmann, T.; Kumari, B.; Zhao, L.; Breitzke, H.; Schöttner, S.; Rüttiger, C.; Gallei, M. Dynamic Nuclear Polarization Signal Amplification as a Sensitive Probe for Specific Functionalization of Complex Paper Substrates. *J. Phys. Chem. C* **2017**, *121*, 3896−3903.

(48) Harrach, M. F.; Drossel, B.; Winschel, W.; Gutmann, T.; Buntkowsky, G. Mixtures of Isobutyric Acid and Water Confined in Cylindrical Silica Nanopores Revisited: A Combined Solid-State NMR and Molecular Dynamics Simulation Study. *J. Phys. Chem. C* **2015**, *119*, 28961−28969.

(49) Vyalikh, A.; Emmler, T.; Gedat, E.; Shenderovich, I.; Findenegg, G. H.; Limbach, H. H.; Buntkowsky, G. Evidence of Microphase Separation in Controlled Pore Glasses. *Solid State Nucl. Magn. Res.* **2005**, *28*, 117−124.

(50) Vyalikh, A.; Emmler, T.; Shenderovich, I.; Zeng, Y.; Findenegg, G. H.; Buntkowsky, G. H-2-Solid State NMR and Dsc Study of Isobutyric Acid in Mesoporous Silica Materials. *Phys. Chem. Chem. Phys.* **2007**, *9*, 2249−2257.

(51) Guo, X.-Y.; Watermann, T.; Sebastiani, D. Local Microphase Separation of a Binary Liquid under Nanoscale Confinement. *J. Phys. Chem. B* **2014**, *118*, 10207−10213.

(52) Melnikov, S. M.; Höltzel, A.; Seidel-Morgenstern, A.; Tallarek, U. Composition, Structure, and Mobility of Water−Acetonitrile Mixtures in a Silica Nanopore Studied by Molecular Dynamics Simulations. *Anal. Chem.* **2011**, *83*, 2569−2575.

(53) Rodriguez, J.; Elola, M. D.; Laria, D. Polar Mixtures under Nanoconfinement. *J. Phys. Chem. B* **2009**, *113*, 12744−12749.

(54) Schmitz, R.; Müller, N.; Ullmann, S.; Vogel, M. A Molecular Dynamics Simulations Study on Ethylene Glycol-Water Mixtures in Mesoporous Silica. *J. Chem. Phys.* **2016**, *145*, No. 104703.

(55) Phan, A.; Cole, D. R.; Striolo, A. Preferential Adsorption from Liquid Water—Ethanol Mixtures in Alumina Pores. *Langmuir* **2014**, *30*, 8066−8077.

(56) Elamin, K.; Jansson, H.; Kittaka, S.; Swenson, J. Different Behavior of Water in Confined Solutions of High and Low Solute Concentrations. *Phys. Chem. Chem. Phys.* **2013**, *15*, 18437−18444.

(57) Elamin, K.; Jansson, H.; Swenson, J. Dynamics of Aqueous Binary Glass-Formers Confined in MCM-41. *Phys. Chem. Chem. Phys.* **2015**, *17*, 12978−12987.

(58) Schirò, G.; Cupane, A.; Pagnotta, S. E.; Bruni, F. Dynamic Properties of Solvent Confined in Silica Gels Studied by Broadband Dielectric Spectroscopy. *J. Non-Cryst. Solids* **2007**, *353*, 4546−4551.

(59) Swenson, J.; Elamin, K.; Chen, G.; Lohstroh, W.; Sakai, V. G. Anomalous Dynamics of Aqueous Solutions of Di-Propylene Glycol Methylether Confined in MCM-41 by Quasielastic Neutron Scattering. *J. Chem. Phys.* **2014**, *141*, No. 214501.

(60) Swenson, J.; Elamin, K.; Jansson, H.; Kittaka, S. Why Is There No Clear Glass Transition of Confined Water? *Chem. Phys.* **2013**, *424*, 20−25.

(61) Vyalikh, A.; Emmler, T.; Grünberg, B.; Xu, Y.; Shenderovich, I.; Findenegg, G. H.; Limbach, H. H.; Buntkowsky, G. Hydrogen Bonding of Water Confined in Controlled-Pore Glass 10−75 Studied by H-1-Solid State NMR. *Z. Phys. Chem.* **2007**, *221*, 155−168.

(62) Grünberg, B.; Emmler, T.; Gedat, E.; Shenderovich, I.; Findenegg, G. H.; Limbach, H. H.; Buntkowsky, G. Hydrogen Bonding of Water Confined in Mesoporous Silica MCM-41 and SBA-15 Studied by H-1 Solid-State NMR. *Chem. - Eur. J.* **2004**, *10*, 5689−5696.

(63) Zang, J.; Konduri, S.; Nair, S.; Sholl, D. S. Self-Diffusion of Water and Simple Alcohols in Single-Walled Aluminosilicate Nanotubes. *ACS Nano* **2009**, *3*, 1548−1556.

(64) Zhao, D.; Feng, J.; Huo, Q.; Melosh, N.; Fredrickson, G. H.; Chmelka, B. F.; Stucky, G. D. Triblock Copolymer Syntheses of Mesoporous Silica with Periodic 50 to 300 Angstrom Pores. *Science* **1998**, *279*, 548−552.

(65) Buntkowsky, G.; Sack, I.; Limbach, H. H.; Kling, B.; Fuhrhop, J. Structure Elucidation of Amide Bonds with Dipolar Chemical Shift NMR Spectroscopy. *J. Phys. Chem. B* **1997**, *101*, 11265−11272.

(66) Sinha, N.; Schmidt-Rohr, K.; Hong, M. Compensation for Pulse Imperfections in Rotational-Echo Double-Resonance NMR by Composite Pulses and Exorcycle. *J. Magn. Reson.* **2004**, *168*, 358−365.

(67) Wilfried Temperature-Dependent Lle in the Non-Miscible Binary System Octanol/Water, 2014. https://de.wikipedia.org/wiki/Octanol-Wasser-Verteilungskoeffizient.

(68) Bennett, A. E.; Rienstra, C. M.; Auger, M.; Lakshmi, K. V.; Griffin, R. G. Heteronuclear Decoupling in Rotating Solids. *J. Chem. Phys.* **1995**, *103*, 6951−6958.

(69) Jorgensen, W. L.; Maxwell, D. S.; Tirado-Rives, J. Development and Testing of the Opls All-Atom Force Field on Conformational Energetics and Properties of Organic Liquids. *J. Am. Chem. Soc.* **1996**, *118*, 11225−11236.

(70) Lindahl, E.; Hess, B.; van der Spoel, D. Gromacs 3.0: A Package for Molecular Simulation and Trajectory Analysis. *J. Mol. Model.* **2001**, *7*, 306−317.

(71) Schuler, L. D.; Daura, X.; van Gunsteren, W. F. An Improved Gromos96 Force Field for Aliphatic Hydrocarbons in the Condensed Phase. *J. Comput. Chem.* **2001**, *22*, 1205−1218.

(72) Berendsen, H. J. C.; Grigera, J. R.; Straatsma, T. P. The Missing Term in Effective Pair Potentials. *J. Phys. Chem.* **1987**, *91*, 6269−6271.

(73) Geske, J.; Vogel, M. Creating Realistic Silica Nanopores for Molecular Dynamics Simulations. *Mol. Simul.* **2017**, *43*, 13−18.

(74) Gulmen, T. S.; Thompson, W. H. Testing a Two-State Model of Nanoconfined Liquids: Conformational Equilibrium of Ethylene Glycol in Amorphous Silica Pores. *Langmuir* **2006**, *22*, 10919−10923.

(75) Hill, J. R.; Sauer, J. Molecular Mechanics Potential for Silica and Zolite Catalysts Vased on Ab Initio Calculations. 1. Dense and Microporous Silica. *J. Phys. Chem.* **1994**, *98*, 1238−1244.

(76) Daniel Berthelot "Sur le mélange des gaz", Comptes rendus hebdomadaires des séances de l'Académie des Sciences, 126 pp. 1703−1855 (1898).

(77) Lorentz, H. A. Ueber Die Anwendung Des Satzes Vom Virial in Der Kinetischen Theorie Der Gase. *Ann. Phys.* **1881**, *248*, 127−136.

(78) Feller, S. E.; Zhang, Y.; Pastor, R. W.; Brooks, B. R. Constant Pressure Molecular Dynamics Simulation: The Langevin Piston Method. *J. Chem. Phys.* **1995**, *103*, 4613−4621.

(79) Phillips, J. C.; Braun, R.; Wang, W.; Gumbart, J.; Tajkhorshid, E.; Villa, E.; Chipot, C.; Skeel, R. D.; Kalé, L.; Schulten, K. Scalable Molecular Dynamics with Namd. *J. Comput. Chem.* **2005**, *26*, 1781−1802.

(80) Limbach, H.-H.; Tolstoy, P. M.; Pérez-Hernández, N.; Guo, J.; Shenderovich, I. G.; Denisov, G. S. Oho Hydrogen Bond Geometries and NMR Chemical Shifts: From Equilibrium Structures to Geometric H/D Isotope Effects, with Applications for Water, Protonated Water, and Compressed Ice. *Isr. J. Chem.* **2009**, *49*, 199−216.

(81) Hartnig, C.; Witschel, W.; Spohr, E.; Gallo, P.; Ricci, M. A.; Rovere, M. Modifications of the Hydrogenbond Network of Liquid Water in a Cylindrical Sio2 Pore. *J. Mol. Liq.* **2000**, *85*, 127−137.

(82) Albert, K.; Bayer, E. Characterization of Bonded Phases by Solid-State NMR Spectroscopy. *J. Chromatogr. A* **1991**, *544*, 345−370.

(83) Björklund, S.; Kocherbitov, V. Alcohols React with MCM-41 at Room Temperature and Chemically Modify Mesoporous Silica. *Sci. Rep.* **2017**, *7*, No. 9960.

(84) García-Antón, J.; Axet, M. R.; Jansat, S.; Philippot, K.; Chaudret, B.; Pery, T.; Buntkowsky, G.; Limbach, H.-H. Reactions of Olefins with Ruthenium Hydride Nanoparticles: NMR Characterization, Hydride Titration, and Room-Temperature C-C Bond Activation. *Angew. Chem., Int. Ed.* **2008**, *47*, 2074−2078.

(85) Mittermaier, A.; Kay, L. E. Measurement of Methyl 2h Quadrupolar Couplings in Oriented Proteins. How Uniform Is the Quadrupolar Coupling Constant? *J. Am. Chem. Soc.* **1999**, *121*, 10608−10613.

(86) Trébosc, J.; Wiench, J. W.; Huh, S.; Lin, V. S. Y.; Pruski, M. Solid-State NMR Study of MCM-41-Type Mesoporous Silica Nanoparticles. *J. Am. Chem. Soc.* **2005**, *127*, 3057−3068.

(87) Pafong, E.; Geske, J.; Drossel, B. On the Influence of the Intermolecular Potential on the Wetting Properties of Water on Silica Surfaces. *J. Chem. Phys.* **2016**, *145*, No. 114901.